Sand wave migration in an anchorage area in the Southern North Sea

L.L. Dorst
Royal Netherlands Navy, Hydrographic Service, The Hague, The Netherlands &
University of Twente, Water Engineering and Management, Enschede, The Netherlands

P.C. Roos, F.M. van der Meer & S.J.M.H. Hulscher
University of Twente, Water Engineering and Management, Enschede, The Netherlands

ABSTRACT: The analysis of a series of offshore bathymetric surveys provides insight into the morphodynamics of the sea floor, which helps to improve resurvey policies for nautical charting. We show results for the anchorage area Maas West in front of the port of Rotterdam, the Netherlands. Our method is based on statistical testing theory, and particularly aimed at the detection of dynamics in tidal sand wave patterns. It results in parameter estimates for the sand wave dynamics, and their uncertainty. Hereto, the area is divided into 18 smaller areas. The results show that a sand wave pattern is detected for many areas, and a shoreward migration is detected for a majority of the areas. The migration rate of the sand waves is up to 7.5 m/yr, with a 95% confidence interval that depends on the regularity of the pattern. The migration rate strongly correlates with the bed level, for which we deduce a linear relation, including its uncertainty. This correlation is in agreement with earlier publications for the Southern North Sea.

1 INTRODUCTION

The sea floor of shallow seas is dynamic. For example, rhythmic morphological patterns on sandy beds can change height and migrate (Wright 1992, Terwindt 1971), thereby possibly endangering navigation through busy shipping lanes. Such patterns exist on many scales (Knaapen et al. 2001). In this paper we consider tidal sand waves, which are characterised by a wavelength of hundreds of meters, a height of several meters, and a migration rate of up to several meters per year. The evolution of the sea floor can be interpreted from a time series of echo sounder surveys, as has been attempted by many authors (recently e.g. Dorst et al. 2006, Knaapen 2005, Van Dijk & Kleinhans 2005). The stochastic character of surveyed depth values of the sea floor complicates the analysis of its evolution: even modern survey techniques reveal depth with an uncertainty of a few decimeters at best (Wells & Monahan 2002), due to random errors in the measurement processes.

Frequent bathymetric surveys of shallow seas are necessary to produce reliable nautical charts. The analysis of past surveys aids the planning of resurvey frequencies. Examples of survey plans are given by De Oliveira et al. (2007), Dehling (2006), Whatrup et al. (2005), and Dorst (2004). Resurvey planning is best served by a method that can separate true sea floor deformation from measurement inaccuracies, and establish whether a new survey confirms previous surveys.

The description of the uncertainty of surveyed depths is a subject of growing interest in the hydrographic community (e.g. Calder 2006, Dorst 2004), since dealing with uncertainties is crucial to control the quality of the survey process and to interpret bathymetric data. Therefore, the method recognizes the stochastic character of surveys.

An overview of general literature on deformation analysis is given by Chrzanowski (2006). This type of analysis applies statistical adjustment theory and testing theory to a series of surveys of deformable objects. We follow the approach of De Heus et al. (1994). Details about the method are given in Dorst et al. (in prep.). A comparison with the approach of Wüst (2004) is given by Lindenbergh et al. (2007).

The anchorage area Maas West has a relatively high resurvey frequency of once per two years. This frequency is based on its location next to an intensively used shipping lane, in combination with its rather shallow depth of 10 to 20 m. To investigate whether the resurvey frequency could be reduced, the five available surveys, measured between 1994 and 2006, were used in a deformation analysis. The results are presented in this paper.

The proposed method is briefly explained in Section 2. The results for the anchorage area Maas West are discussed in Section 3. Sections 4 and 5 contain the discussion and conclusions, respectively.

2 METHODS

2.1 *Input requirements*

Deformation analysis uses statistical testing theory (e.g. Koch, 1999) to analyze time series of surveys. When applied to the sea floor, we use depth values at the nodes of a grid, the uncertainty of each depth value and the time of each survey. The grid is identical for each survey. The uncertainty describes the combined effect of all the measurement and processing errors. Possible sand wave patterns are assumed to be regular, such that a horizontal direction of the pattern variation can be identified as the *x*-direction of the grid, perpendicular to the direction of along-crest uniformity, which is the *y*-direction of the grid. The grid spacing has to be dense enough with respect to the wavelength of the sand wave, to prevent aliasing effects.

2.2 *Selection of parameters*

The depth and uncertainty data are used to estimate parameters using a linear least-squares procedure. These parameters describe the morphology of the sea floor and its dynamics. Hereto, the sea floor can be represented at different levels of complexity. The determination of the spatial complexity is phase 1, and the dynamics are found in phase 2.

In phase 1, the initial characterisation is a horizontal plane, which is extended with spatial parameters that are regarded significant. The extensions are formulated as statistical hypotheses. One hypothetical extension is a sloping plane, using the parameters bed level, slope in *x*-direction and slope in *y*-direction. It is selected if the sea floor is significantly sloping, according to a statistical testing procedure. If a statistically significant sand wave pattern is present, a second hypothetical extension is selected, which is a plane superimposed by a sine wave. The sine wave has a wavelength corresponding to the wavelength that fits best to the data, or dominant wavelength. The additional parameters are sand wave amplitude and phase. Wavelength is considered invariant, both spatially over the area considered, and temporally for all surveys. The significant parameters are input for the deformation analysis, in phase 2.

From the dynamical behavior of the input data, phase 2 derives bed level change, sand wave growth and sand wave migration. We express growth as a percentage of amplitude, because the relative change in height of our characterisation corresponds to the relative change in height of the true morphology. The migration rate is defined as the change in phase times the dominant wavelength.

To find parameter dynamics, we specify two kinds of extensions, which are used as statistical hypotheses again. The extensions are a linear trend in all surveys and a single outlying survey, and they apply to both all planar parameters and all sand wave parameters. These hypothetical extensions are illustrated in Figure 1. The method starts by assuming a static sea floor characterisation at the selected level of complexity, and continues by adding extensions to this characterisation, to model the dynamics by a combination of the hypothetical extensions. For every extension a statistical hypothesis is set up, and a corresponding test statistic and critical value are calculated. Each test statistic is divided by its critical value, to obtain a test quotient q for that extension. The critical values depend on the levels of significance, which represent the probability that the extension is accepted, while it is in fact not present. Those levels of significance need to be set by the user. The most significant addition to the characterisation has the highest test quotient q. That most significant extension is added to the characterisation, if q is larger than one.

2.3 *Calculation of morphological uncertainty*

The iterative addition of extensions continues until there are no extensions accepted anymore. If the characterisation fits the dynamic behavior of the series of surveys well enough, from a statistical point of view, the final parameter values are calculated, as well as their associated uncertainties. The test applied for this decision is called the overall test.

However, if the differences between the characterisation and the sea floor are larger than can be explained by the uncertainty of Section 2.1, the characterisation is insufficient. The differences are called the residuals. Instead of defining additional hypothetical parameters, which make the characterisation more complicated, we assume the residual variation is a random function, and add it to the uncertainty as additional morphological variance and covariance components, using Least Squares Variant Component Estimation (LSVCE) (Teunissen & Amiri-Simkooei, 2007).

The approach described in this subsection is followed for both the phases. A larger uncertainty for the input data of those less regular areas in phase 2 means that it is less likely that an extension will be accepted in that phase. Also, it means that the resulting dynamic parameter will be estimated less accurately for those areas. At the end of phase 2, the second LSVCE procedure only influences the final uncertainty of the estimated parameters.

2.4 *Application to the anchorage area*

The sea floor at the anchorage area has a rhythmic pattern of 200 to 375 m length, which are the limits of the wavelength interval that we use to detect sand waves. This is for instance visible in the 20 m depth line of Figure 2. Waves of about 1 km length are also visible in the same directions, and shoreface-

connected ridges with a wavelength of several kilometres can be identified as well. Since these larger patterns are not the focus of this study, we limit the size of the analysis areas to about a square kilometre. In this way, the dynamics on these scales will be reflected by a change in detected bed level or slope.
A grid spacing of 50m is sufficient to capture the sand wave pattern. This spacing allows for an area size of about one by one kilometer on an ordinary computer, which gives us eighteen areas, denoted A to R (Figure 2). The levels of significance are of great importance for the correct detection of extension. They are set as 5% in phase 1, and 7% for trends and 5% for outliers in phase 2, as explained in Dorst et al. (in prep.).

3 RESULTS

3.1 *Properties of the surveyed areas*

The direction of the sand wave pattern, perpendicular to the crests, is approximately Northeast/Southwest for all areas (Figure 3). This direction was determined using the DIGIPOL method (RIKZ 1997), which calculates variability values for a series of directions. The DIGIPOL-quotient between the value for the direction of highest variability and the value for the direction of lowest variability determines the strength of the preference for that direction. Figure 4 shows the spatial variation per area by its 95th percentile, around a fitted sloping plane. The Northwestern areas seem to have the largest pattern. This Figure also shows the bed level of each area, resulting from phase 2.

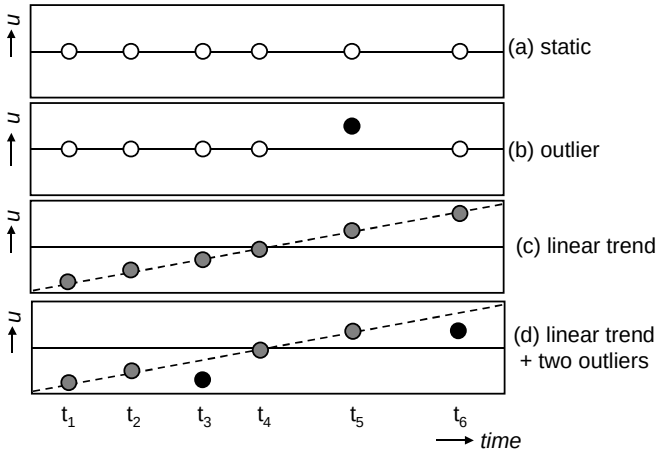

Figure 1. Sketches for dynamics of the parameters. (a) static; (b) an outlier; (c) a linear trend; (d) a combination of a linear trend and two outliers.

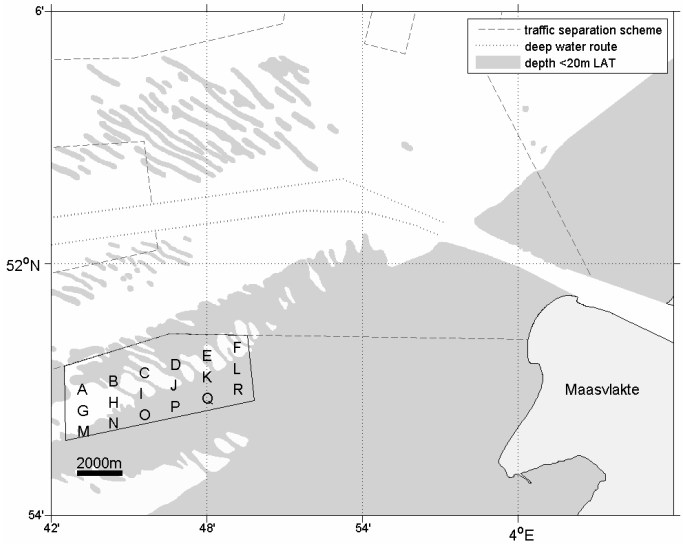

Figure 2. Anchorage area Maas West, consisting of eighteen smaller areas A to R. The Maasvlakte is the most seaward area of the port of Rotterdam.

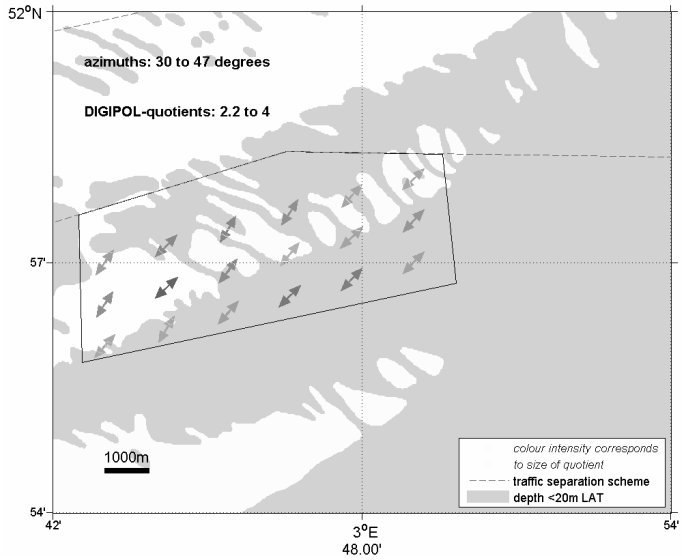

Figure 3. Pattern direction and quotients between value for direction of highest variability and value for direction of lowest variability, according to DIGIPOL, as applied to the December 1994 survey (darker is larger).

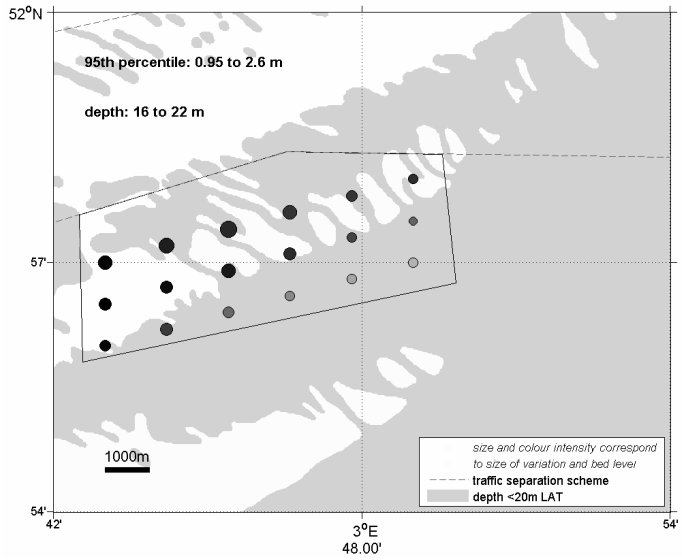

Figure 4. Bed level (intensity of the circles, darker is deeper) and 95th percentiles of the spatial variation (size of the circles,

larger is more variation), as applied to the December 1994 survey.

Five surveys of this area are available, measured in December 1994, May 1996, April 2000, January 2003 and February 2006 by ships of the Hydrographic Service. All depth values used have been reduced to the Lowest Astronomical Tide level (LAT). The horizontal coordinates have all been transformed to the local grid system. These coordinates were originally in the geodetic datum WGS84, in UTM31-projection. The first four surveys were done using a single-beam echo-sounder (SBES), and the last survey was done using a multi-beam echo-sounder (MBES).

The initial variances are the sum of the measurement variances and the interpolation variances. Measurement variance of the SBES surveys is modelled a priori for the survey ships of the Hydrographic Service, according to Dorst (2004). Interpolation variances are given by the universal Kriging procedure that is applied for the interpolation. For the MBES survey, no interpolation is necessary, since the depth value at the grid node is simply selected. For this survey, the measurement variance of IHO publication S44, 4th edition, Order 1, is used (International Hydrographic Organisation, 1998). For a depth of about 20 m, this results in an initial variance of about 0.25 m^2 (which is about 1 m at a 95% confidence level), for both the SBES surveys and the MBES survey.

The initial measurement covariances are modelled using a two-dimensional Gaussian function, with inflection points set at 2500 m in the direction of the ship track, and 50 m across-track. The covariance for small distances is 0.01 m^2, which accounts for the uncertainty of the water level reduction, the largest correlated error in the measurement process. This corresponds to an uncertainty in water level reduction of 0.2 m at a 95% confidence level.

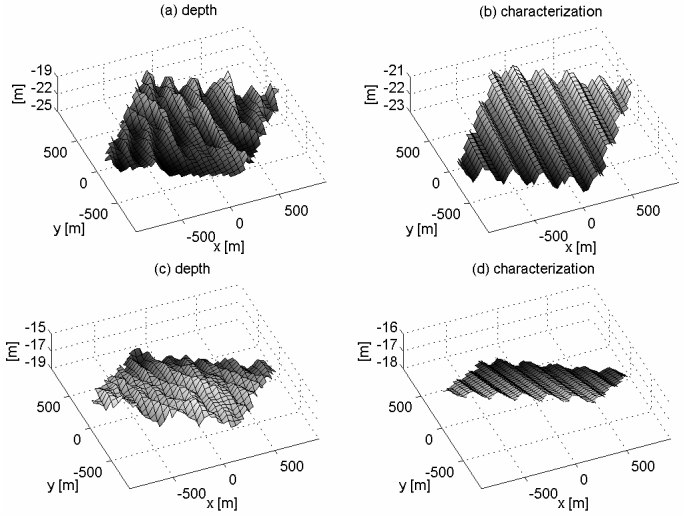

Figure 5. Depth values and characterisation for areas H and Q: (a) gridded depth values under Lowest Astronomical Tide for area H; (b) characterisation after phase 1 for area H; (c) gridded depth values under Lowest Astronomical Tide for area Q; (d) characterisation after phase 1 for area Q. All values are averages over the five surveys. Note that the vertical axes have been exaggerated.

3.2 *Global results of all areas*

The procedure detects fifteen areas that are regular enough to approximate by a sand wave pattern with a constant wavelength. Examples are given in Figure 5. All detected sand waves of phase 1 are given in Figure 6. The amplitudes of the estimated sine functions are smaller than the spatial variations (Figure 4), because of e.g. the asymmetry of the waves, or variations in the crest direction. However, the larger amplitudes in the Northwest correlate with the larger spatial variations in the Northwest. For all areas, the overall test of phase 1 is rejected. Therefore, additional morphological variance is added to the uncertainty of the depth data.

The results of phase 2 are given in Figure 8 and Table 1. Sand wave dynamics are found for eleven areas. All those sand wave dynamics are linear trends, no outliers were found for the sand wave behavior. As indicated by Table 1, the trends were detected because of a migration. The average migration rate is 4.2 m/yr. The growth of the amplitudes is not significant, as the estimates are much smaller than the 95%-values of the confidence intervals.

No migration was detected for four of the fifteen sand wave areas, because the LSVCE procedure in phase 1 has added too much morphological variance for the residuals to the uncertainty of the depth data. This makes the testing process of phase 2 less powerful, by reducing the test quotients. In the case of those four areas, the test quotients q were reduced to a value below one.

An overview of the pattern of all areas where migration was found, is given in Figure 7, ordered from a small to a large migration rate. Some of the wave-crests disappear in areas F and K, resulting in a dominant wavelength that is larger than the maximum of the specified interval. Those disappearing crests are the cause of the 1 km scale pattern visible in the 20 m depth line of Figure 2. In those two figures, a sand wave was spuriously detected. A further observation of Figure 7 is that the wavelength seems to decrease with an increasing migration rate.

The effect of migrating sand waves on depth is a decrease in depth at one side of the sand waves. The depth at such a location keeps decreasing, until the crests has passed. The danger to shipping that this involves is shown in Figure 9. If an analysis is done per grid node, the only spatial parameter involved is depth. Often, linear trends are detected for those nodes that are located on a slope of a sand wave crest. These trends can have a size of up to 0.5 m/yr upward for the anchorage area.

The uncertainty of the migration rate depends on the additional morphological variance as well, and thereby on the regularity of the pattern. For instance,

the most accurate migration rate is found for area H, which has the largest DIGIPOL-quotient (Figure 3). Area H also has a relatively large amplitude (Figure 6), in spite of its relatively small spatial variation (Figure 4). The depth values and characterisation of area H are given in Figure 5a. It is studied in detail in Section 3.3.

The Southeastern areas migrate faster than average: the largest migration rate found is 7.5 m/yr, for area Q. This shallow area has a small dominant wavelength and a small amplitude (Figures 4 and 6). The small amplitude is caused by a small spatial variation (Figure 4), not by high irregularity of the pattern, see its DIGIPOL-quotient, which is about average (Figure 3). The depth values and characterisation of area Q are given in Figure 5b.

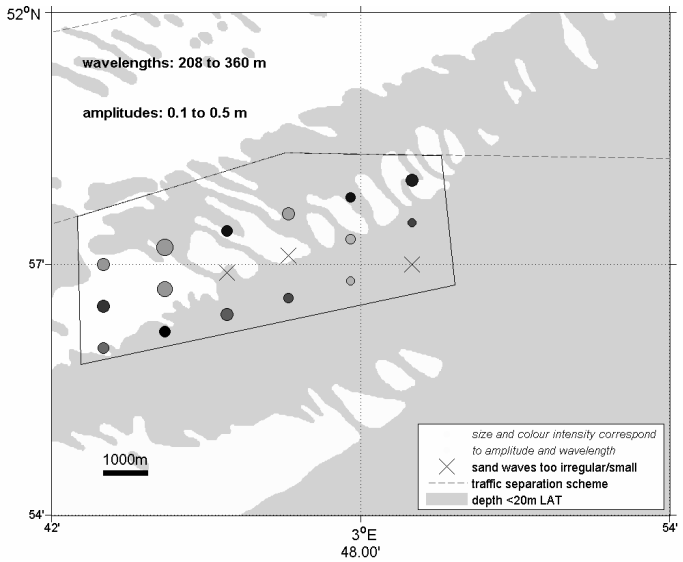

Figure 6. Results of phase 1: detected dominant wavelengths (intensity of the circles, darker is larger wavelength) and their fitted amplitudes (size of the circles, larger is larger amplitudes).

Table 1. Linear trends for sand wave dynamics per area. The values and their 95%-confidence intervals are given. A-F: Northern; G-L: central; M-R: Southern.

Area	Sand wave growth		Sand wave migration rate	
	value [%/yr]	CI [%/yr]	value [m/yr]	CI [m/yr]
A	+1.6	9.1	+3.7	3.1
B	+0.1	6.3	+3.6	2.3
C	-	-	-	-
D	-1.1	8.1	+4.5	3.1
E	-	-	-	-
F	+1.5	5.3	+3.1	2.6
G	-1.3	6.2	+4.7	3.3
H	+0.3	4.6	+2.4	1.6
I	no sand wave pattern detected			
J	no sand wave pattern detected			
K	+3.5	8.0	+3.1	2.2
L	-	-	-	-
M	+1.5	7.3	+3.6	2.9
N	-	-	-	-
O	+0.8	6.4	+5.1	2.7
P	+2.3	9.8	+5.6	4.2
Q	+2.5	6.5	+7.5	1.9
R	no sand wave pattern detected			

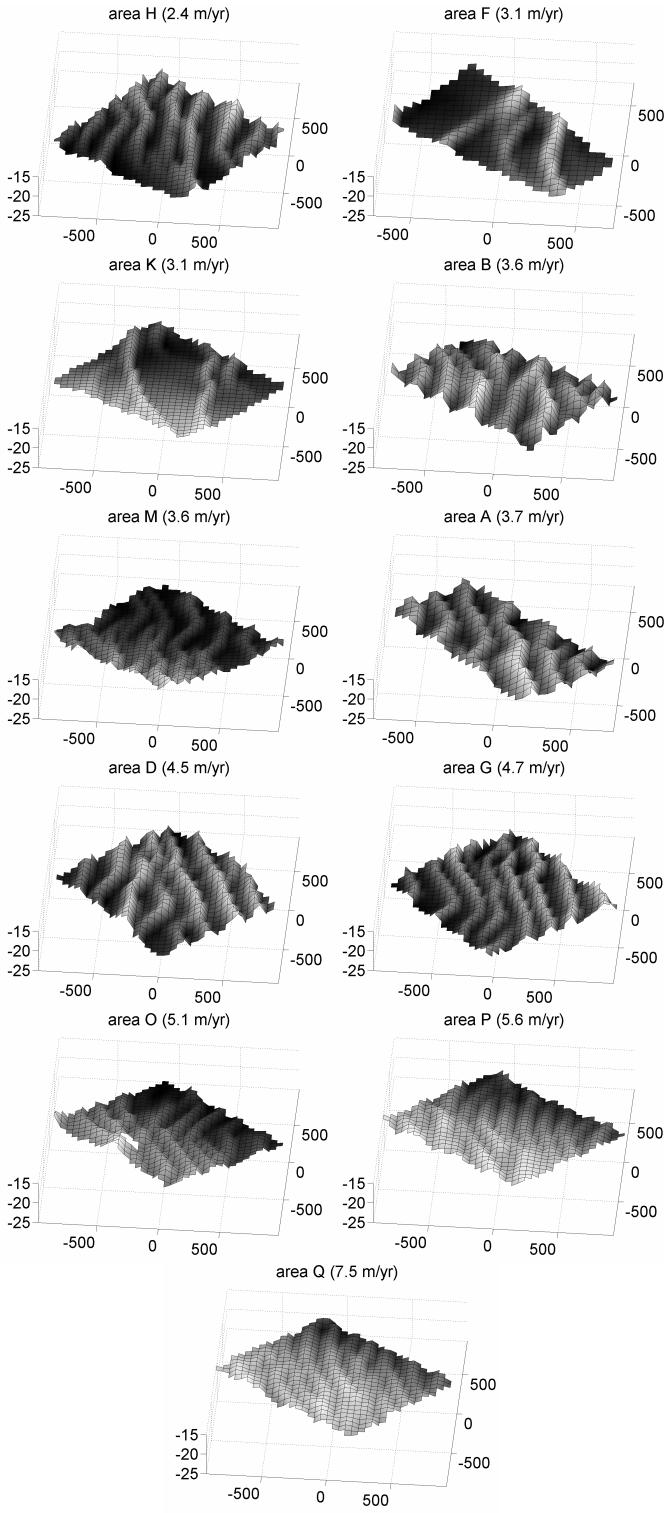

Figure 7. Depth values and migration rate for all areas where migration is detected, ordered from small migration rate estimates to large estimates.

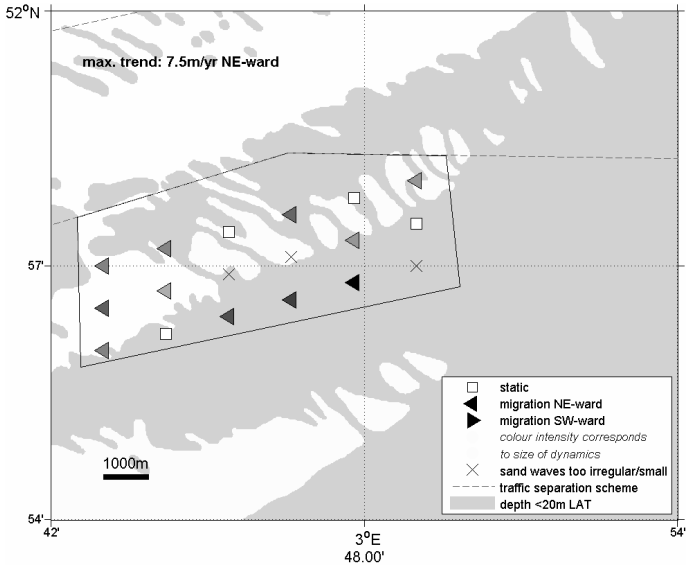

Figure 8. Results of phase 2: migration (darker is larger migration rate)

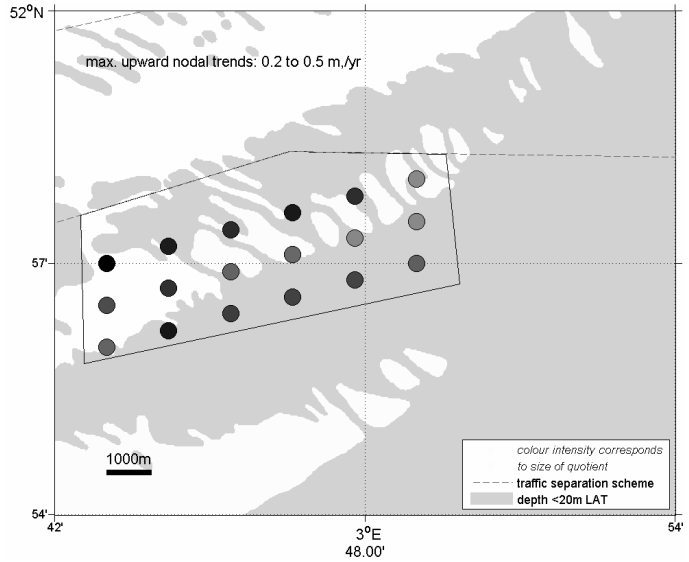

Figure 9. Maximum upward linear trends in depth, detected at individual grid nodes (darker is larger trend).

3.3 *Detailed results of area H*

Area H deserves a more detailed study, as it has the most accurate results. Figure 10 shows the resulting parameters of phase 1 using the white circles. Both a slope in the plane and a sand wave pattern were detected, as the test quotients q for both these extensions are larger than one (Figure 11). Therefore, five parameters per survey are used.

The black circles show the results after phase 2. The planar results are static, and the sand wave results show the trend. The vertical lines and the crosses indicate the 95% confidence intervals of the results of phase 1 and phase 2, respectively. In this phase, the results are described by three planar static parameters, two sand wave parameters for the first survey, and two sand wave trend parameters.

The differences between the planar estimates of phase 1 and the static planar estimates of phase 2 are so small that the differences are not significant, hence the initial static characterisation is accepted. The sand wave results of phase 2 show a clear migration, which is detected by the procedure. The amplitude obtained in phase 2 is smaller than the amplitude obtained in phase 1. As there are fewer parameters, it is harder to adapt the phase 2 representation to the actual situation, causing the sand wave pattern to fit less well. The worse fit becomes apparent by the smaller amplitude of the pattern.

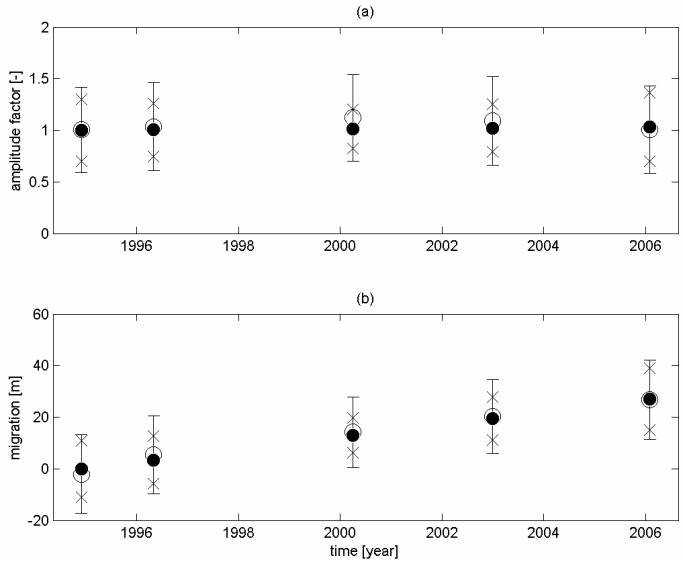

Figure 10. Sand wave results for area H, for a dominant wavelength of 231 m and a reference amplitude of 0.38 m: (a) sand wave growth; (b) sand wave migration. The white circles are the results after phase 1, and the black circles indicate linear trend, found in phase 2. The variations that phase 1 shows are approximated by the phase 2 results, which are exactly on a sloping line. The trends of phase 2 are 0.3%/yr, and 2.4 m/yr for (a) and (b) respectively. The vertical lines and the crosses indicate the 95% confidence intervals of the results of phase 1 and phase 2, respectively.

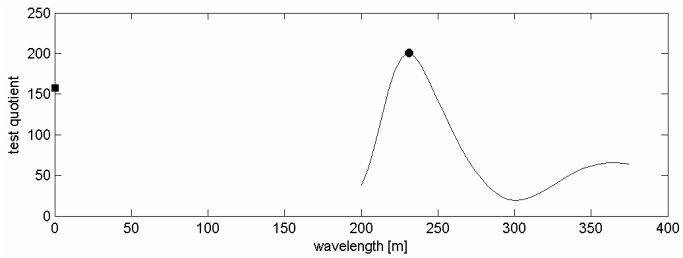

Figure 11. Test quotients q for phase 1 of area H: square at vertical axis: test quotient for slopes; line: test quotients for sand waves as function of wavelength, and for planar extension at zero wavelength; circle: maximum test quotient, corresponding to the dominant wavelength of 231 m.

It is clear that the confidence intervals of phase 2 are smaller than those of phase 1. There are less parameters in phase 2, while the number of depth values at the input side stays the same. As the amount of data per parameter increases, the results become more accurate.

The results of an analysis per grid node confirms the observed migration (Figure 12). At one side of the crests, downward trends are found, and at the other side, there are upward trends.

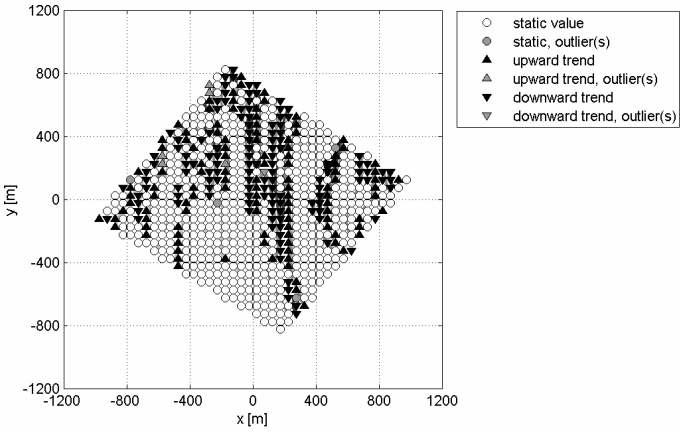

Figure 12. Dynamics detected at the individual grid nodes of area H. The trends have values up to 0.35 m/yr, and the outliers up to 1.8 m.

4 INTERPRETATION OF MIGRATION RATES

4.1 *Introduction*

Migration of observed sand waves in the Southern North Sea has been studied before, recently e.g. by Knaapen (2005) and Van Dijk & Kleinhans (2005). Knaapen (2005) finds a correlation between migration rates and the three parameters sand wave lee/stoss asymmetry, the square of wavelength, and the inverse of waveheight, for migration rates up to 10 m/yr, while Van Dijk & Kleinhans (2005) report for coastal sites that migration rates up to 20 m/yr exist, depending on depth. Process-based models confirm these migration rates for the Southern North Sea (Németh et al. 2002, Besio et al. 2004).

In Section 4.2, we study if there is a correlation between migration rate and depth, wavelength, and waveheight. Hereto, we use the bed level estimate (Figure 4), the dominant wavelength (Figure 6), and the spatial variation (Figure 4), respectively. In Section 4.3, we explore if there is a relation with asymmetry for the anchorage area Maas West. In Section 4.4, we make a comparison with some process-based results.

4.2 *Correlations with bed level, wavelength and spatial variation*

We use the estimates and uncertainties for the migration rates c in linear regressions with bed level d, dominant wavelength L and spatial variation v, obtaining expressions:

$$c = a_d\, d + b_d,$$
$$c = a_L\, L^2 + b_L,$$
$$c = a_v\, /v + b_v.$$

The estimates for migration rate are plotted against these three variables in Figure 12, including the 95% confidence intervals for migration rate. The resulting linear correlations are also given in Figure 12, and in Table 2. Table 2 shows the correlation coefficients as well.

We assume the bed level estimates are deterministic, because their 95% confidence intervals are very small: 0.07 m, on average. The correlation coefficients reveal there is a strong correlation with bed level, a mild correlation with spatial variation, and hardly any correlation with the dominant wavelength.

As we have seen in Section 3.2, the sand wave patterns of areas F and K are in fact not showing a wavelength in the specified range. To study their effect, we exclude the two areas, and calculate the correlations again. The results are again given in Figure 12 and Table 2. Now, the correlation with spatial variation becomes stronger, and the correlation coefficients with the other two variables hardly change.

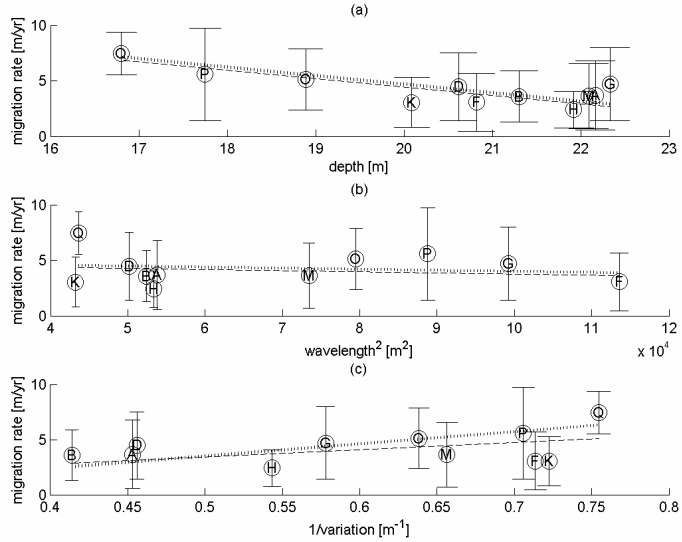

Figure 12. Estimation of a linear correlation between migration rate and (a) bed level; (b) dominant wavelength; and (c) spatial variation, based on all areas where migration is detected. The dashed lines include all migrating areas, and the dotted lines exclude the areas F and K.

Table 2. Correlation estimates a, b of migration rate u with bed level d, dominant wavelength L and spatial variation v, their uncertainties at a 95% confidence interval, and correlation coefficients (c.c.).

Parameter	a		b		c.c.
	value	CI	value	CI	
including areas F and K:					
d [1/yr; m/yr]	-0.76	0.40	19.7	8.2	-0.78
L^2 [1/(m yr); m/yr]	$1{\cdot}10^{-5}$	$3.4{\cdot}10^{-5}$	4.7	2.3	-0.04
$1/v$ [m²/yr; m/yr]	6.5	6.4	0.1	3.9	0.36
excluding areas F and K:					
d [1/yr; m/yr]	-0.76	0.40	20.1	8.2	-0.84
L^2 [1/(m yr); m/yr]	$1{\cdot}10^{-5}$	$5.2{\cdot}10^{-5}$	4.9	3.2	0.05
$1/v$ [m²/yr; m/yr]	11.0	7.2	-2.0	4.2	0.61

4.3 *Influence of asymmetry*

Unfortunately, the current implementation of the estimation procedure does not provide for an asymme-

try parameter. A mathematical assessment of the correlation is therefore not possible. To circumvent this problem, we could order the graphs of the observed depth values of each area where migration is detected, from small migration rate estimates to large estimates (Figure 7). An increase or decrease in visible asymmetry is an indication that the two are correlated.

Most of the areas show lee/stoss asymmetry, confirming the predictive power of this asymmetry for migration. The relation between the strength of asymmetry and the migration rate is not clear from Figure 7.

4.4 *Comparison to process-based results*

The process-based model of Németh et al. (2002) has been further developed by Van den Berg & Van Damme (2006) and Van der Meer et al. (2007). For a depth d of 20 m and a maximum depth averaged tidal stream of 0.5 m/s, we define three scenarios. They are no residual current (scenario 1), a residual current of 0.05 m/s (scenario 2), and a residual current of 0.1 m/s (scenario 3). Scenario 1 gives a wavelength L of 300 m, and scenario 2 and 3 of 270 m. The migration rate c of scenario 1 to 3 is 0 m/yr, 1-2 m/yr and 5-7 m/yr, respectively. According to the model, the amplitude grows up to at least 10 m, within two decades.

The observed migration confirms the results of the scenarios that involve a residual current, taking into account its uncertainty (Figure 8 and Table 1). Scenario 2 and 3 correspond to the minimum and maximum observed migration rate, respectively.

5. CONCLUSION

The anchorage area Maas West shows migration rates up to 7.5 m/yr, which causes decreasing depths, and thereby endangers navigation and anchoring. The migration rate is larger in the shallower areas in the South-East. This confirms the dependency on depth, assumed by Van Dijk & Kleinhans (2005), and is also explained by process-based models, like Németh et al. (2002). Deformation analysis allows us to estimate a linear relation, including its uncertainty, which allows for a proper comparison with observations of others and process-based models. To ensure safe navigation and anchorage in the approach to the port of Rotterdam, it is important that this dynamic area is surveyed at the high frequently of once every two years.

6. ACKNOWLEDGMENTS

This project has been co-sponsored by the Technology Foundation STW, the applied science division of NWO, and the technology program of the Dutch Ministry of Economic Affairs.

7. REFERENCES

Besio, G., P. Blondeaux, M. Brocchini & G. Vittori. 2004. On the modelling of sand wave migration. *J. of Geophysical Res. - Earth Surfaces* 109 (C04108), doi: 10.1029/2002JC001622.

Calder, B. 2006. On the uncertainty of archive hydrographic surveys. *IEEE Journal of Oceanic Engineering* 31(2): 249-265, doi: 10.1109/JOE.2006.872215.

Chrzanowski, A. 2006. *Tasks and achievements of the FIG working group on deformation measurements and analysis, Proceedings of the 3rd IAG symposium on Geodesy for geotechnical and structural engineering and 12th FIG symposium on deformation measurement, Baden, Austria*. Vienna University of Technology, Austria. Available via www.fig.net/commission6/baden_2006/proceedings.htm.

Dehling, T. 2006. Determining survey frequency and resolution, BSH concept and realisation. *Hydro Int.* 10(2): 7-9.

De Heus, H., P. Joosten, M. Martens & H. Verhoef. 1994. Stability analysis as part of the strategy for the analysis of the Groningen gasfield levellings. In H. Papo (ed.), *Proceedings of the Perelmutter workshop on dynamic deformation models, Haifa, Israel, 29 August – 1 September 1994.*

De Oliveira, S.S., F. Mandarino & F.J.D. Souza. 2007. FIS: re-survey decision system – using fuzzy inference systems for area selection. *Hydro Int.* 11(3): 31-34.

Dorst, L.L. 2004. Survey plan improvement by detecting sea floor dynamics in archived echo sounder surveys. *Int. Hydrographic Rev., New Series* 5(2): 49-63.

Dorst, L.L., P.C. Roos & S.J.M.H. Hulscher. 2007. Estimation of sand wave dynamics in the Southern North Sea. In J. McKee Smith (ed.), *Proceedings of the 30th International Conference on Coastal Engineering, San Diego, 3-8 September 2006*. Singapore: World Scientific Publishing.

Dorst, L.L., P.C. Roos & S.J.M.H. Hulscher. In prep. The estimation of sea floor dynamics from bathymetric surveys of a sand wave area. To be published in *J. of Geophysical Res. - Earth Surfaces.*

Duffy, G. P. & J. E. Hughes-Clarke. 2005. Application of spatial cross correlation to detection of migration of submarine sand dunes. *J. of Geophysical Res. - Earth Surfaces* 110, no. F04S12, doi: 10.1029/2004JF000192.

International Hydrographic Organisation. 1998. IHO standards for hydrographic surveys. Special publication S44, 4th ed. Monaco: International Hydrographic Bureau. Available via www.iho.int.

Knaapen, M.A.F. 2005. Sandwave migration predictor based on shape information. *J. of Geophysical Res. - Earth Surfaces* 110, no. F04S11, doi: 10.1029/2004JF000195.

Knaapen, M.A.F., S.J.M.H. Hulscher & H. J. de Vriend. 2001. A new type of sea bed waves, *Geophysical Res.. Letters* 28(7), 1323-1326.

Koch, K.-R. 1999. *Parameter estimation and hypothesis testing in linear models*. 2nd ed., Berlin: Springer-Verlag.

Lindenbergh, R.C., L.L. Dorst, J.C. Wüst & P.G. Menting. 2007. Simulation, detection and prediction of sea floor dynamics. *International Hydrographic Review, New Series* 8(2): 25-36.

Németh, A. A., S.J.M.H. Hulscher & H.J. de Vriend. 2002. Modelling sand wave migration in shallow shelf seas. *Continental Shelft Res.* 22: 2795-2806.

RIKZ. 1997. *Gebruikershandleiding DIGIPOL*. The Hague: Rijkswaterstaat, Rijksinstituut voor Kust en Zee.

Terwindt, J.H.J. 1971. Sand waves in the southern bight of the North Sea. *Marine Geology* 10: 51-67.

Teunissen, P.J.G. & A.-R. Amiri-Simkooei. 2007. Least squares variance component estimation. *J. of Geodesy* 11, doi:10.1007/s00190-007-0157-x.

Van den Berg, J. & Van Damme, D. 2006. Sand wave simulations on large domains. In G. Parker & M.H. Garcia (eds.) *Proceedings of the 5th IAHR symposium on River, Coastal & Estuarine Morphodynamics, Urbana, Illinois, United States.*

Van der Meer, F.M., S.J.M.H. Hulscher & D.M. Hanes & E. Elias. 2007. San Fransisco Bay sand waves: modelling and observations. In C.M. Dohmen-Janssen & S.J.M.H. Hulscher (eds.) *Proceedings of the 6th IAHR symposium symposium on River, Coastal & Estuarine Morphodynamics, Enschede, The Netherlands.*

Van Dijk, T. A. G. P. & M. G. Kleinhans. 2005. Processes controlling the dynamics of compound sand waves in the North Sea, Netherlands *J. of Geophysical Res. - Earth Surface*s 110, no. F04S10, doi: 10.1029/2004JF000173.

Wüst, J.C. 2004. Data-driven probabilistic predictions of sand wave bathymetry. In S.J.M.H. Hulscher, T. Garlan & D. Idier (eds.), *Proceedings of the 2nd international workshop on marine sandwave and river dune dynamics, Enschede, The Netherlands, 1-2 April 2004.*

Wells, D. E. & D. Monahan. 2002. IHO S44 standards for hydrographic surveys and the variety of requirements for bathymetric data. *The Hydrographic J.* 104: 9-15.

Whatrup, C., D. Mann & B. Davidson. 2005. The UK civil hydrography programme - Changing the mould. *Int. Hydrographic Rev. - New Series* 6(2): 45-56.

Wright, P. 1992. Long term changes to the positions and heights of sandwaves in the southern North Sea. *Int. Hydrographic Rev.* 69(2): 113-128.